

## GPU-based, parallel-line, omni-directional integration of the acceleration field to obtain the 3D pressure distribution

Jin Wang<sup>1</sup>, Cao Zhang<sup>1</sup> and Joseph Katz<sup>1</sup>

<sup>1</sup> Department of Mechanical Engineering, Johns Hopkins University, Baltimore, USA

### Abstract

For recent years, PIV based pressure reconstruction from material acceleration either by solving Pressure Poisson Equation (PPE) or by direct integration has been studied. The advantage of direct integration on no need of prescribed pressure boundary encourage us to develop a 3D direct integration method. In this paper, a GPU-based, parallel-line, omni-directional integration (Omni3D) method has been developed and tested using the JHU DNS Database, comparing with three different methods. In a series of tests, Omni3D tends out to be a robust and efficient method with only 1 minute for one realization. This method is also utilized to compute the volumetric pressure in a turbulent channel flow over a compliant surface.

**Keywords:** turbulence; pressure measurement;

### Introduction

PIV-based pressure measurement techniques involving direct integration of material acceleration or solving the Pressure Poisson Equation (PPE) have become popular in recent years. While PPE can be readily extended to volumetric measurements [1] using e.g. time-resolved tomographic PIV data [3], extension of the direct integration method, such as the 2D Virtual-boundary Omni-directional integration (Omni2D, [2]) from 2D to 3D, has been problematic owing to the massive amount of computations involved. Yet, omni-direction integration is effective in minimizing the effect of local acceleration errors. Hence, our goal is to develop and evaluate a fast and robust 3D pressure reconstruction method.

### The 3D GPU-based Parallel-line Omni-directional integration method

The new GPU-based, parallel-line, omni-directional method (Omni3D) integrates the material acceleration along a series of parallel lines aligned in all possible directions. These directions are determined by a spherical virtual grid that surrounds the sample volume. The pressure at every point is the average value obtained from all the paths crossing this point. Hence, errors associated with a certain path are minimized. Iterations (3-4) are used for correcting the initially assumed pressure distribution along the external surfaces of the sample volume. Hence, there is no need to prescribe a boundary condition. Methods for identifying and circumventing regions with particularly high material acceleration errors have also been developed.

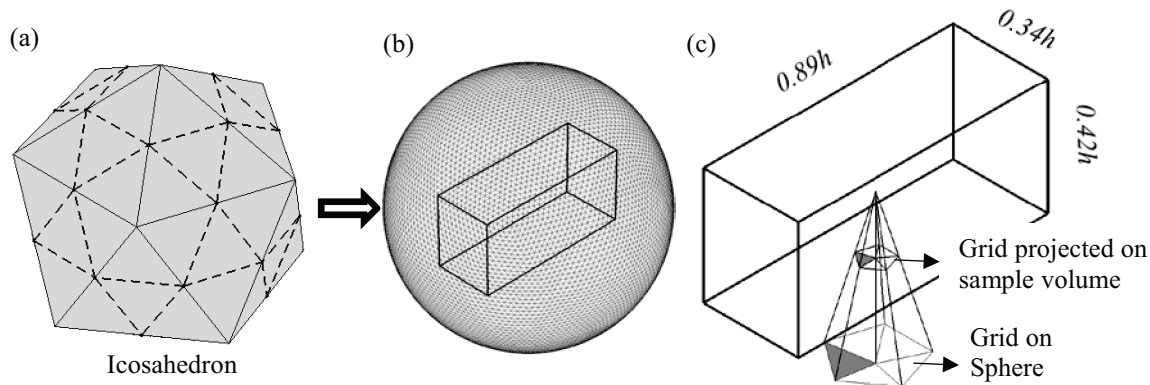


Figure 1 The grid with 20480 surfaces used for generating the parallel line integration paths.

To assure the grid homogeneity, an initially icosahedron grid is divided recursively several times, as illustrated in Figure 1. In each step each triangular surface is divided to four parts and projected onto the surface of the sphere. Repeating this procedure 6 times generates a spherical triangular grid with 20480 faces (Figure 1(b)). As illustrated in Figure 1(c), the projected area from each spherical virtual surface should match the data resolution, yielding  $4\pi(L/2)^2/N_f \sim 0.5\Delta x^2$ , where  $L$  is the length of the sample volume ( $4\pi/3(L/2)^3=V$ ,  $V$  is the volume),  $\Delta x$  is the data resolution, and  $N_f$  is the number of triangular

faces. Hence,  $N_f \sim 3 \times 10^4$  for a grid of  $100 \times 47 \times 38$  voxels, the grid of our recent TPIV measurements. For the present  $N_f = 20480$ , the resulting total number of integration paths is in the order of  $10^8$ , requiring more than 3 hours for integrating the acceleration in a single realization using a 3.7 GHz, 8 core Intel i7-3770k processor. This computing time is reduced to about one minute by implementing the same integration algorithm on a low cost, Tesla K40c GPU board, which has 2880 745 MHz processors.

The detailed computation steps are presented in Figure 2:

Step.1 Allocate memory needed on GPU device. Read acceleration data and transfer it to the GPU memory. The total memory needed is 3 GB.

Step.2 Use parallel-line omni-directional integration (PLODI) in parallel to obtain the pressure difference between every two different boundary nodes, denoted as  $PINT(nin, nout)$ , where,  $nin$  is the integration path starting point and  $nout$  is the integration path ending point. Subsequently, parallel boundary pressure iteration is performed with the known pressure difference using

$$p_{nout}^{new} = \frac{\sum_{nin=1, nin \neq nout}^N (p_{nin}^{old} + PINT(nin, nout))}{N - 1}$$

It can be verified that this iteration scheme is equivalent to a least square fit of the overdetermined linear system.

Step.3 In parallel, assign each thread an integration path to perform PLODI to obtain the pressure at inner nodes. The inner pressure is the averaged results of all the integration paths.

Step.4 Transfer pressure data from device to host and write it to the disk.

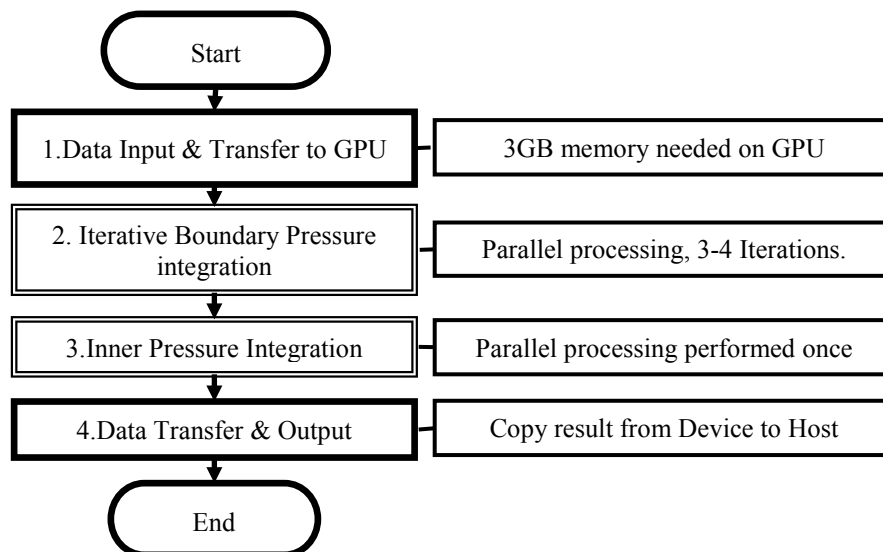


Figure 2 The flow chart of Omni3D Method

### DNS Verification of Omni3D

The pressure predicted by the Omni3D method is compared to several other procedures, such as planar integration using Omni2D combined by planar integration along a perpendicular plane (Omni2D), as well as by solving the PPE with Dirichlet boundary conditions on one surface. These conditions are obtained either using the Bernoulli equation (PPE-Bernoulli [1]) or Omni2D integration along this surface (PPE-Omni2D). Validations are performed using the JHU DNS database for turbulent channel flow [4]. Randomly distributed synthetic particles are generated and displaced by the velocity field obtained from database. Subsequently, velocities are calculated via cross correlation using different interrogation volume (I.V.) ranging from 5 wall units to 20 wall units. Volume pressure is reconstructed from the material accelerations obtained by Lagrangian method [2], using four different methods.

As illustrated in Figure 3(a), for error-free acceleration (SVD Interpolation), the Omni3D and PPE-Omni2D give nearly identical results for the entire flow field, whose RMS error of  $p^+$  is below 0.15. The PPE-Bernoulli results are erroneous in the vicinity of the Dirichlet boundary, but this error diminishes with increasing distance from this surface, becoming very small on the opposing surface, consistent with [1]. The Omni2D errors are substantially higher due to limited components of accelerations and much less number of integration paths. With larger amount of errors in acceleration (Figure 3(a)), Cross

Correlation, I.V. =10 wall units), both Omni3D and PPE-Omni2D keep the pressure errors locally high near the wall. The large error near the wall is due to significant velocity gradient and large interrogation volume there. The reduction of cross correlation interrogation volume can greatly reduce those errors from 1.3 to 0.1 at  $y^+=5$ , as illustrated in Figure 3(b).

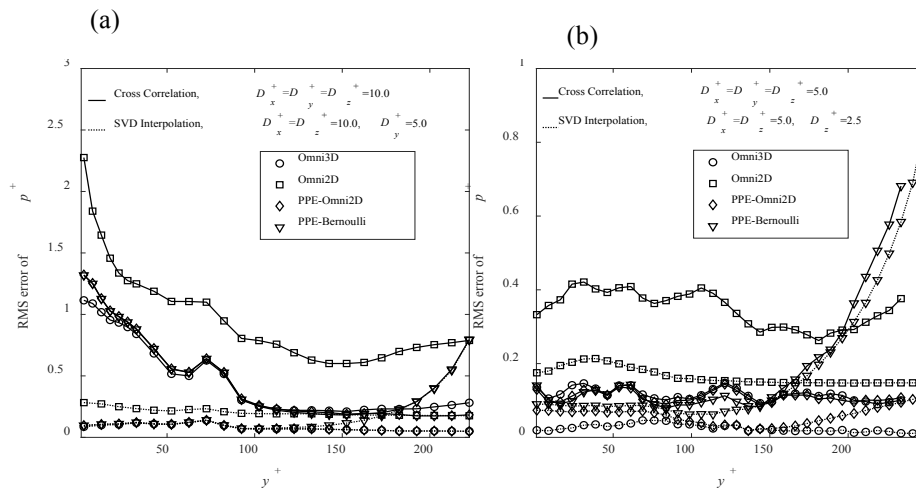


**Figure 3** RMS error of pressure resulting from integration of acceleration obtained from cross correlation and SVD interpolation.

The Omni3D method can be further improved by incorporating prior knowledge about the spatial distribution of acceleration uncertainty. Firstly, 100% additive noise is added to the accelerations in the high error zone (HEZ). In the selected-path method, paths carrying error from HEZ to LEZ is circumvented while in the weighted-path method, each path is given a weight which is inversely proportional to the path dependent mean of curl of acceleration. In Figure 4(c), when there is no additive noise, the separation of HEZ and LEZ is done by setting a threshold for the curl of accelerations. In Figure 4(b), the advanced methods clearly reduced the error both in LEZ and HEZ and presented a sharp separation of pressure error between them. In Figure 4(c), error near the wall in further reduced by using the advanced methods.

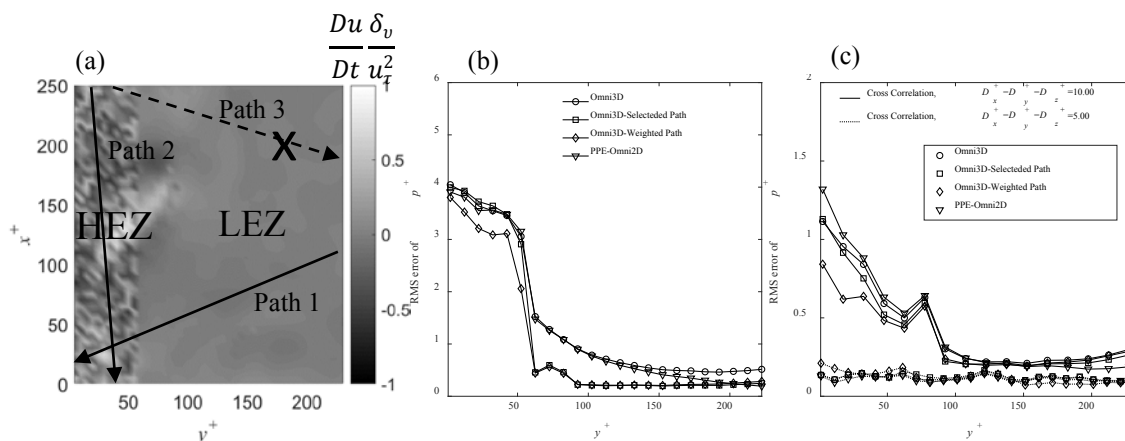


**Figure 4** Error propagation in a channel flow. (a) Location of randomly distributed 100% error in acceleration, (b) effect of selected paths and  $\nabla \times \frac{Du}{Dt}$  weighted paths on error propagation in (a), (c) effect of selected paths and  $\nabla \times \frac{Du}{Dt}$  weighted paths on error propagation in synthetic PIV.

### Application of Omni3D on Turbulent Channel Flow over a Compliant Surface

The Omni3D method has been utilized to reconstruct the measured 3D pressure field in a turbulent channel flow over a compliant surface at  $Re_\tau=2300$  [5]. The time-resolved 3D velocity distributions have been measured using TPIV, and the 2D surface deformation by the Mach-Zender Interferometry (MZI) integrated into the TPIV system. The material acceleration is calculated by a Lagrangian method [2]. Pressure field is reconstructed via four different methods. Combined plots of velocity

vector, contour lines of  $\lambda_2 (< -2e4 \text{ 1/s}^2)$  and pressure fluctuations are illustrated in Figure 5. We clearly see that low pressure peaks at the vortex core and high pressure peaks at the interface of sweep ejection transition, which is consistent with our previous findings [5]. Among the four methods, Omni2D has significant higher magnitude of pressure peaks and it's worse than others if we scrutinize the pressure RMS profiles. The correlations of deformation and pressure (not shown here) can tell us that Omni3D method yields the highest correlation values.

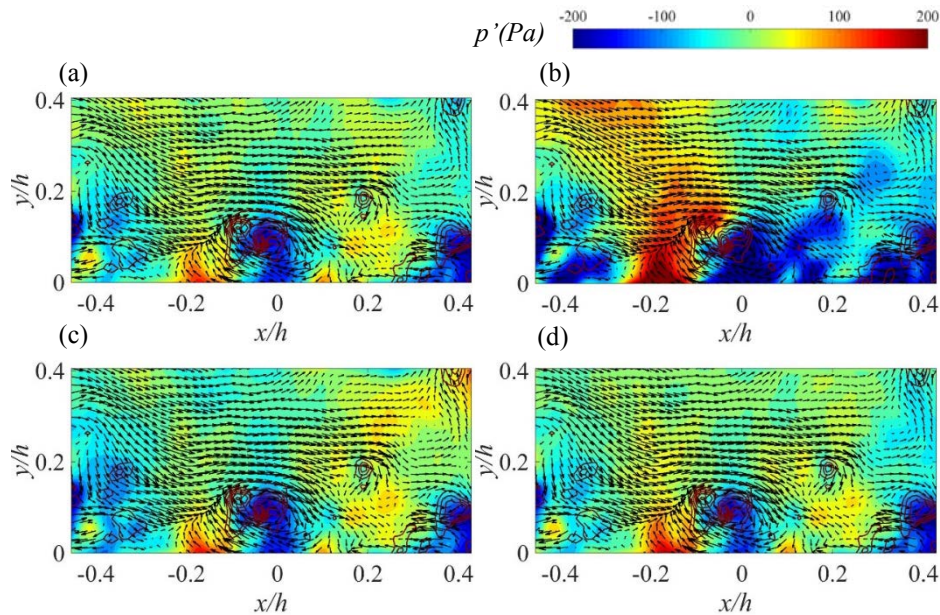


Figure 5 Instantaneous pressure field, velocity vectors and contour line of  $\lambda_2 (< -2e4 \text{ 1/s}^2)$  at  $x$ - $y$  plane of four integration methods. (a) Omni3D, (b) Omni2D, (c) PPE-Omni2D, (d) PPE-Bernoulli.

### Conclusion

In our work, a GPU-Based fast 3D parallel-line Omni-directional integration method is established for calculation of 3D pressure distribution. The method is compared with three other methods. The new method shows the outstanding capability of obtaining accurate pressure field based on the DNS verification and experimental applications. The advantage of Omni3D lies in no need of boundary condition, parallel computing features, as well as incorporating known acceleration uncertainty information to minimize error propagations.

### References

- [1] S. Ghaemi and F. Scarano, 2013. *Turbulent Structure of High-Amplitude Pressure Peaks within the Turbulent Boundary Layer*, Journal of Fluid Mechanics, 735, 381–426;
- [2] Xiaofeng Liu and Joseph Katz, 2006. *Instantaneous Pressure and Material Acceleration Measurements Using a Four-Exposure PIV System*, Experiments in Fluids, 41.2 (2006), 227–40;
- [3] G. E. Elsinga and others, 2005. *Tomographic Particle Image Velocimetry*, 6th International Symposium on Particle Image Velocimetry, 1–12;
- [4] J. Graham and others, 2016. *A Web Services-Accessible Database of Turbulent Channel Flow and Its Use for Testing a New Integral Wall Model for LES DNS Approach and Simulation Parameters*. Journal of Turbulence, 17.2 (2016), 181–215;
- [5] Cao Zhang, Jin Wang, William Blake and Joseph Katz, 2016. *Deformation of Compliant Wall in Trubulent Channel Flow*, Journal of Fluid Mechanics;